

1 Thermal and radiation response of 4H-SiC 2 Schottky diodes with direct-write electrical 3 contacts

5 Cite as: Appl. Phys. Lett. **116**, 000000 (2020); doi: 10.1063/5.0007496

6 Submitted: 16 March 2020 · Accepted: 6 June 2020 ·

7 Published Online: 0 Month 0000



View Online



Export Citation



CrossMark

9
10 Neil R. Taylor,^{1,2} Yongchao Yu,¹ Mihee Ji,¹ Tolga Aytug,¹ Shannon Mahurin,¹ Richard Mayes,¹ Sacit Cetiner,¹
11 M. Parans Paranthaman,¹ Dianne Ezell,¹ Lei R. Cao,² and Pooran C. Joshi^{1,a)}

12 AFFILIATIONS

13 ¹Oak Ridge National Laboratory, 1 Bethel Valley Road, Oak Ridge, Tennessee 37830, USA

14 ²Nuclear Engineering, Department of Mechanical and Aerospace Engineering, The Ohio State University, 201 W. 19th Ave,
15 Columbus, Ohio 43210, USA

16 ^{a)}Author to whom correspondence should be addressed: joshipc@ornl.gov

ABSTRACT

17 A high-sensitivity 4H-SiC temperature sensor and an alpha detector have been fabricated using additively printed metal contacts. The sur-
18 face morphology and electrical conductivity of the printed electrodes were established prior to Schottky diode development. 4H-SiC
19 Schottky diodes with direct-write printed silver contacts on the 5 μm-thick epilayer on 4H-SiC were characterized electrically in terms of the
20 forward and reverse current-voltage and high-frequency capacitance-voltage characteristics. The turn-on voltage of the Schottky diodes,
21 as established from the forward current-voltage characteristics measured up to a temperature of 400 °C, showed a linear temperature
22 dependence. Schottky diodes with direct-write printed Ag electrodes were able to measure alpha particles emitted from Americium-241. The
23 high temperature and radiation response of the Schottky diodes show their suitability for multi-modal sensor fusion on the 4H-SiC platform
24 for harsh environment applications.

Published under license by AIP Publishing. <https://doi.org/10.1063/5.0007496>

25 Highly linear temperature sensing instruments are important for
26 almost all industrial and research applications. Industries such as
27 aerospace, automotive, drilling, and nuclear all have interest in the
28 development of advanced temperature sensors.¹⁻⁴ Within the nuclear
29 industry, next generation of reactors is of great interest, and advanced
30 sensors are required that can operate in harsh environments to achieve
31 the desired safety and reliability. Thermocouples, resistance tempera-
32 ture detectors (RTDs), optical fibers, and semiconductor diodes are all
33 possible solutions to provide robust high temperature sensing capabili-
34 ties. Among the various temperature sensor types, semiconductor
35 diode-based sensors offer the advantage of cointegration of sensors
36 and integrated circuits (ICs).⁵

37 Wide bandgap (WBG) silicon carbide (SiC) offers a unique com-
38 bination of structural, composition, and electrical characteristics for
39 high temperature, high frequency, and harsh environment applica-
40 tions. It offers a wide bandgap (3.23 eV for 4H) compared to that of
41 silicon (1.12 eV), as well as a high melting point (2730 °C), which
42 allows it to operate at much higher temperatures than silicon. High
43 thermal conductivity (3–5 W/cm K) and high breakdown field

strength (2.0 MV/cm) of SiC material make it attractive for high power
and high voltage applications.⁶ SiC has been extensively studied, and
fabrication techniques have been developed which allow for the high-
quality crystal growth using chemical vapor deposition (CVD) of
substrates and epitaxial layers. It has also been demonstrated to func-
tion in a wide variety of sensor modalities such as radiation, gas, tem-
perature, and optical sensors.^{4,7,8} Semiconductor-based temperature
sensors have been fabricated and demonstrated on 4H-SiC^{5,9,10} using
microelectronic processing techniques. In the present work, we report
on the direct-write printing of Ohmic and Schottky contacts to fabri-
cate 4H-SiC-based temperature sensors and radiation detectors for
advanced nuclear applications.

Typical fabrication of a semiconductor diode using microelec-
tronics processing techniques involves device patterning using a mask
and photolithography. After photolithography, the photoresist is
developed and then metal is typically deposited by sputtering or
electron-beam evaporation techniques. A final liftoff step is completed
to remove excess metal and photoresist. The cleanroom fabrication
does not lend itself well to rapid prototyping of sensor designs for

63 specific applications or integration scheme and requires the fabrication
 64 of photomasks for each sensor design one would want to produce.
 65 Even for a single layer design, the cleanroom fabrication can take
 66 hours to fabricate a set of sensors, while direct-write printing allows
 67 the fabrication of these detectors in under an hour depending on the
 68 design scheme. As is the focus of the present work, the digital direct-
 69 write printing technique allows selective deposition of a material
 70 without the usage of a mask.¹¹ It also enables a fast printing of neutron
 71 convertor materials onto a thin-film semiconductor (e.g., SiC) so that
 72 the conventional two-step process, with the first step being the deposit
 73 metal contact and the second step being coated neutron convertor
 74 materials, into one single step, which will drastically speed up the sen-
 75 sor optimization and final product fabrication time. This process can
 76 print functional material on a substrate such as a ceramic or semicon-
 77 ductor on either a flat or a curved surface with a linewidth control,
 78 which is fast approaching levels below 10 μm with the emerging print-
 79 ing techniques and concepts. The types of materials that can be
 80 printed include metals, polymers, semiconductors, dielectrics, and
 81 adhesives.

82 In this paper, we demonstrate the temperature response and radi-
 83 ation detection characteristics of 4H-SiC Schottky diodes fabricated
 84 using the aerosol jet technique. Silver contacts were printed on 4H-SiC
 85 substrates to form Schottky and Ohmic contacts using nanosilver
 86 conductive inks (Source: Clariant, Prelect TPS 50 G2). The electrical
 87 contacts were printed using an Optomec Aerosol Jet 200 series system
 88 operated in ultrasonic mode to aerosolize the inks into the necessary
 89 mist for printing. As shown in Fig. 1(a), a carrier gas is flown through
 90 the atomizer to pick up the nanoparticles and carry them to the deposi-
 91 tion head. At the deposition head, a second gas, the sheath gas, is used
 92 to focus the nanoparticles through the aerosol nozzle for a controlled
 93 deposition onto the substrate. The printing process is controlled by a
 94 2D/3D motion control system. The desired digital design can be
 95 produced CAD software and filled with the print pattern according to
 96 specific parameters. The program can control the print speed, line

97 overlap, sheath gas flow velocity, carrier gas flow velocity, and number
 98 of printed layers. The gas flow rates and nozzle selection allow for the
 99 adjustment of the printed linewidth and the amount of material depos-
 100 ited. All these parameters affect the overall print quality including the
 101 thickness, coverage, and overspray. Table I lists the typical printing
 102 parameters used for the deposition of silver Schottky contacts.

103 All devices were fabricated on 4H-SiC wafers (source:
 104 NOVAsiC) with a 5-μm-thick epilayer ($n \sim 5 \times 10^{15} \text{cm}^{-3}$) grown
 105 on high-conductivity 4H-SiC ($\rho \sim 0.02 \Omega \text{cm}$). Silver contacts were
 106 printed on both the epitaxial and bulk sides of 13 mm × 13 mm square
 107 dies to form Schottky and Ohmic contacts, as verified by the electronic
 108 characteristics. Circular contacts ranging from diameters of 1–3 mm
 109 were printed on the epitaxial side. On the epitaxial wafer contacts,
 110 additional 0.5 mm diameter silver contact pads were printed on top of
 111 the larger metal contacts. These contact pads were printed to act as a
 112 robust contact point for making electrical connection to the contact
 113 with micropositioners. The wafers were held at a temperature of 70 °C
 114 during printing to aid in the evaporation of the ink solvent. 115
 116 Figure 1(b) shows the printed silver top-contacts in the top right cor-
 117 ner of the left die and the silver Ohmic backside contact on the right
 118 die. The direct-write printing approach allows for multi-material
 119 printing on the same layer. Figure 1(b) demonstrates the possibility of
 120 multi-material printing as attempted for platinum (bottom left), gold
 121 (bottom right), and nickel (top left) contacts. The metal contact
 122 morphology was examined using an Atomic Force Microscope to
 123 determine the thickness and roughness of the printed metal-line. As
 124 shown in Fig. 1(c), the printed metal linewidth is about 30 μm with an
 125 average height of 0.47 μm and an RMS roughness of about 0.13 μm.
 126 The metal lines were overlapped 50% to print the target electrode size.
 127 The printed metal-line showed a high electrical conductivity, as shown in
 128 Fig. 1(d), which improved with an increase in thermal curing tempera-
 129 ture. At a curing temperature of 250 °C, the metal-lines showed a sheet
 130 resistance value below 0.01 Ω/□. The metal conductivity did not change
 131 significantly with a further increase in curing temperature to 300 °C. To
 132 analyze the device characteristics for harsh environment applications, the
 133 temperature-dependent electrical properties of the fabricated Schottky
 134 diodes were evaluated from room temperature up to 400 °C, while radia-
 135 tion detection characteristics were established by exposing to alpha radia-
 136 tion from the Americium-241 (Am-241) emitter of 1.0 μCi.

137 The devices were characterized electrically and tested for temper-
 138 ature sensing capabilities. The samples were placed upon a Signatone
 139 S-1160 Series Probe Station and Signatone S-1060 Hot Chuck. The hot
 140 chuck utilizes a DC power source to supply 0–120 V and 0–7.5 A to
 141 power the hot chuck. The power supply uses a PID Athena microcon-
 142 troller to control the temperature setpoint. The probe station and hot

AQ2

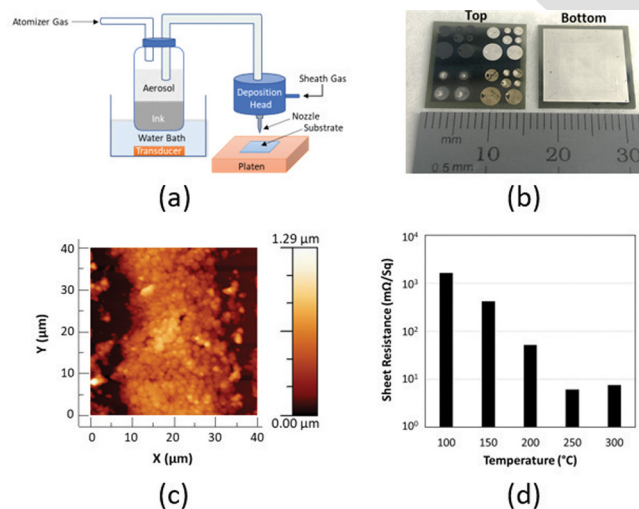


FIG. 1. (a) Schematic of the Aerosol jet printing system, (b) printed Schottky contacts on the 4H-SiC epitaxial side and the Ohmic contact on the bulk side, (c) surface morphology of printed contacts, and (d) printed silver conductivity.

TABLE I. Printing parameters for silver Schottky contacts.

Control parameter	Value
Nozzle diameter	150 μm
Print speed	6 mm/s
Line width	30 μm
Sheath flow	16 sccm
Ultrasonic atomizer flow	50 sccm

143 chuck are housed within a Signatone Dark Box to reduce EM interfer- 160
 144 ence and avoid any current generation from incident light on the 161
 145 device. Micropositioners were used to make connection to the 162
 146 device contacts, and measurements were performed using a Keithley 163
 147 4200 A-SCS Parameter Analyzer to collect forward current-voltage 164
 148 (FIV), reverse current-voltage (RIV), and capacitance-voltage (C-V)
 149 data. These measurements detail the behavior of the device acting as a
 150 diode and determine its capability to act as a temperature sensor and
 151 as a radiation detector.

152 The hot chuck was used to vary the device temperature in the 165
 153 range of 20 – 400 °C to examine the effect of temperature on the elec- 166
 154 trical conductivity characteristics of the Schottky diodes with printed 167
 155 contacts. FIV and RIV measurements were conducted to quantify the 168
 156 turn-on voltage and overall current flow through the device. The turn- 169
 157 on voltage and current flow values at various temperatures were used 170
 158 to determine if the contacts have a linear response to measurement 171
 159 temperature. Figure 2 shows FIV plots across the investigated 172

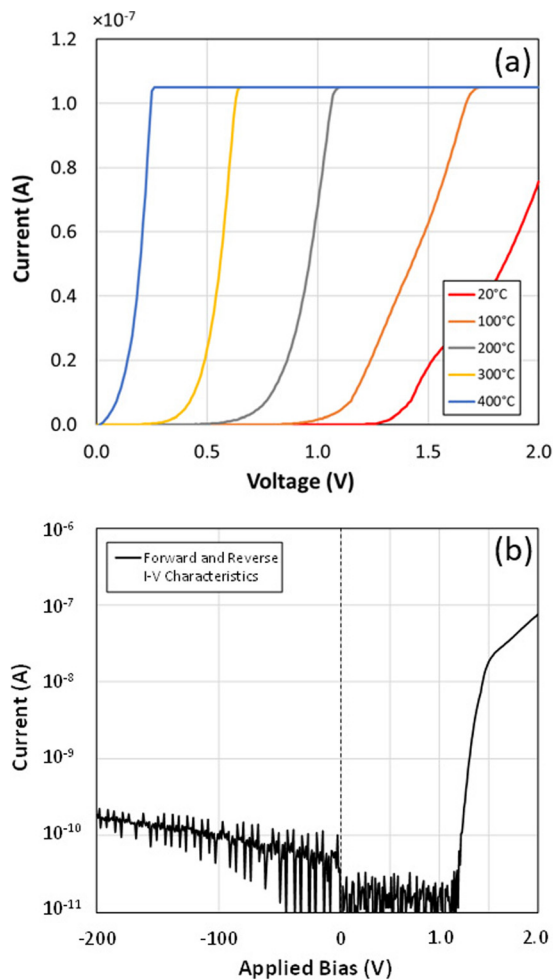


FIG. 2. (a) Temperature dependence of forward electrical conductivity characteristics of Schottky diodes and (b) typical forward and reverse bias characteristics at room temperature.

160 temperature range for a 4H-SiC Schottky diode. The RIV plot at vary- 161
 162 ing temperatures showed a relatively high breakdown voltage exceed- 163
 164 ing –200 V up until the 400 °C measurement. For a semiconductor
 diode, the forward current behavior of the device can usually be sim-
 plified to the thermionic emission theory and follows

$$I = I_s \left(e^{\frac{qV}{nkT}} - 1 \right), \quad (1)$$

165 where q is the electronic charge, V is the applied voltage, n is the ideal- 166
 167 ity factor, k is the Boltzmann constant, T is the temperature, and I_s is 168
 169 the saturation current. The current flowing through the device is 170
 171 highly dependent on the temperature, which forms the basis of the 172
 173 temperature sensor. To accurately determine the turn-on voltage of 174
 175 the diode at these temperatures, a forward current density threshold of 176
 177 $2.83 \times 10^{-7} \text{ A/cm}^2$ was chosen as the turn-on current. The voltage at 178
 179 which each contact reached this current threshold at various tempera- 180
 181 tures is plotted in Fig. 3. A least-squared fitting method was applied 182
 183 to determine the linearity of the I–V response at various temperatures. 184
 185 All the devices, with various electrode diameters in the range of 186
 187 1–3 mm, showed a very linear response with r^2 values greater than 0.9. 188
 189 The calculated sensitivity of these devices was about 3.3 mV/°C. The 190
 high sensitivity of the printed devices matches well with the values
 reported for the devices fabricated by surface micro-machining⁹ and
 thermal evaporation techniques.¹²

High-frequency (1 MHz) capacitance-voltage (C–V) measure-
 ments were conducted on the Schottky diodes to gain an understand-
 ing of the metal/4H-SiC interface. The doping density and Schottky
 barrier height (SBH) can be extracted from the C–V characteristics
 using the following equation:

$$\frac{1}{C^2} = \frac{2}{qN_D\epsilon_s\epsilon_0A^2} (V_{bi} - V), \quad (2)$$

186 where C is the diode capacitance, A is the electrode area, q is the elec- 187
 188 tronic charge, N_D is the doping concentration, ϵ_s is the permittivity of 189
 the semiconductor, ϵ_0 is the permittivity of free space, V_{bi} is the built-
 in potential, and V is the applied bias voltage. The doping density was

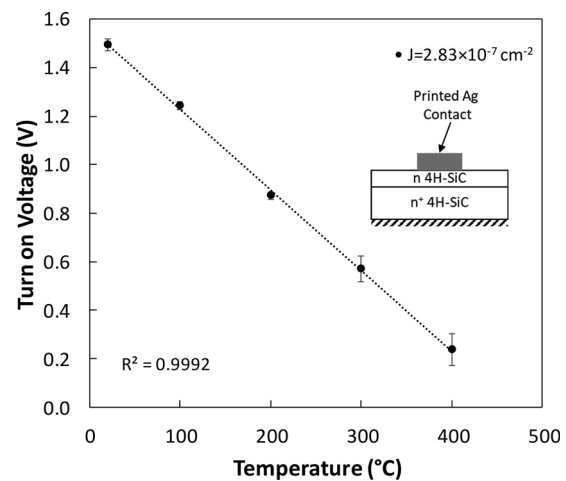


FIG. 3. Turn-on voltage vs temperature response of Schottky diodes with printed silver contacts.

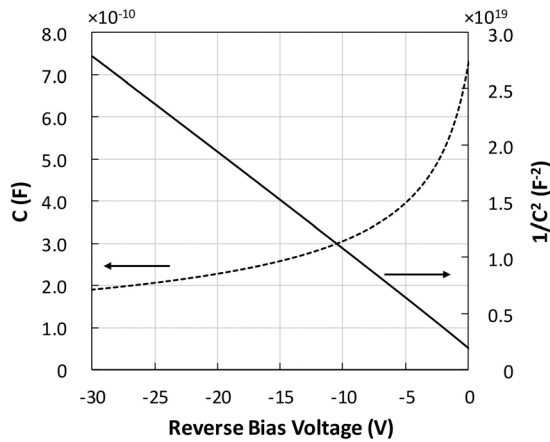


FIG. 4. High frequency capacitance–voltage characteristics of Schottky diodes.

190 calculated from the slope of the $C^{-2} - V$ plot as shown in Fig. 4. The
 191 linearity of the $C^{-2} - V$ plot indicates uniform doping in the depletion
 192 region of the semiconductor. The calculated donor doping concentration
 193 was $3.56 \times 10^{15} \text{ cm}^{-3}$. The built-in potential value, as determined from the
 194 intercept of the $C^{-2} - V$ plot, was found to be 0.41 V.
 195

196 These devices were also tested for their radiation detection capability
 197 to act as a dual-mode sensor. Figure 5 shows the radiation response
 198 of the Schottky diodes measured over a voltage range of up to -220 V .
 199 The devices were tested in a vacuum chamber with a $1 \mu\text{Ci}$ Am-241
 200 button source positioned approximately 2 cm above the detector. The
 201 detector experienced a fluence of approximately $(1.7 \pm 0.1) \times 10^3 \text{ alphas/cm}^2 \text{ s}$.
 202 The energy deposited in the detector continues to increase up to the final
 203 bias voltage of -220 V . The increase in energy deposition and the
 204 subsequent charge collection are attributed to the increase in the bias-
 205 dependent depletion depth, and the induced charge on the metal contact
 206 could be explained by

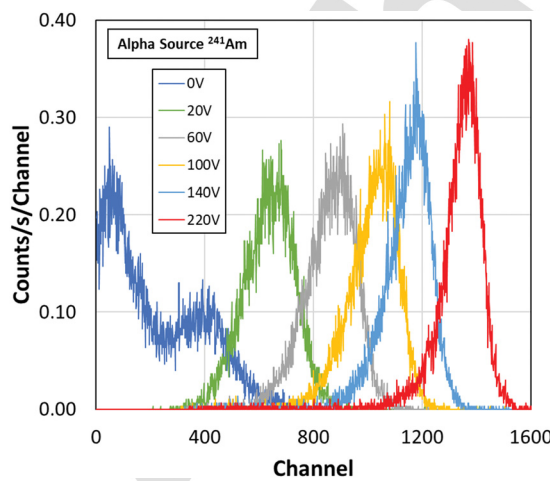


FIG. 5. Alpha spectra of the Am-241 source acquired on Schottky diodes with a 2 mm diameter silver contact at varying bias from 0 to -220 V .

207 proximity sensing,¹³ i.e., charge can be induced on the printed metal
 208 electrode, even if the metal is not physically in contact with the semi-
 209 conductor. The device never reaches saturation due to the depletion
 210 region of the device never reaching the full penetration depth of the
 211 alpha particles. SRIM calculations have shown that the range of a
 212 5.486 MeV alpha particle in SiC is approximately $18.9 \mu\text{m}$. The depletion
 213 depth calculated using the doping concentration and a voltage of
 214 -220 V is less than $7 \mu\text{m}$. The spectral response at zero bias, i.e., vol-
 215 taic mode, however, corroborates the formation of the SBH due to
 216 electronic state Fermi-level pinning at the metal-semiconductor inter-
 217 face¹⁴ or interface dipole formation.¹⁵ The observed alpha-radiation
 218 response shows that a combination of the direct-write printing tech-
 219 nique and 4H-SiC material can be used for multi-modal sensor system
 220 development for high temperature and harsh environment applica-
 221 tions. The radiation response of these detectors can be further tuned
 222 by increasing the epilayer thickness and reducing the epilayer dopant
 223 concentration to fully attenuate the incident alpha particles.

224 Direct-write printing of electrical contacts on 4H-SiC material
 225 shows promise for multimodal sensor development for high tempera-
 226 ture and harsh environment applications. The 4H-SiC Schottky
 227 diodes fabricated using printed silver contacts exhibited excellent on-
 228 state characteristics with a linear temperature response of $3.3 \text{ mV}/^\circ\text{C}$
 229 up to 400°C . The Schottky diodes also showed a clear response to the
 230 alpha source with a Gaussian shape of the peaks as expected from an
 231 alpha particle source. The observed thermal and alpha radiation
 232 responses of 4H-SiC Schottky diodes show the potential of digital
 233 printing techniques for multi-modal sensors and integrated sensor
 234 system development.
 235

236 This research was sponsored by the Laboratory Directed Research
 237 and Development Program of Oak Ridge National Laboratory (ORNL),
 238 managed by UT-Battelle, LLC for the U.S. Department of Energy under
 239 Contract No. DE-AC05-00OR22725. This manuscript was authored by
 240 UT-Battelle, LLC, under Contract No. DE-AC05-00OR22725 with the
 241 U.S. Department of Energy (DOE).
 242

DATA AVAILABILITY

243 The U.S. government retains and the publisher, by accepting this
 244 article for publication, acknowledges that the U.S. government retains
 245 a nonexclusive, paid-up, irrevocable, and worldwide license to publish
 246 or reproduce the published form of this manuscript, or allow others to
 247 do so, for U.S. government purposes. DOE will provide public access
 248 to these results of federally sponsored research in accordance with the
 249 DOE Public Access Plan (<http://energy.gov/downloads/doi-public-access-plan>).
 250

REFERENCES

251
 252 ¹P. Ohodnicki, Jr., S. Credle, M. Buric, R. Lewis, and S. Seachman, "High tem-
 253 perature, harsh environment sensors for advanced power generation systems,"
 254 *Proc. SPIE* **9467**, 94671M (2015).
 255 ²G. Brezeanu, M. Badila, F. Draghici, R. Pascu, G. Pristavu, F. Craciunoiu, and
 256 I. Rusu, "High temperature sensors based on silicon carbide (SiC) devices," in
 257 *International Semiconductor Conference (CAS) (IEEE, 2015)*, pp. 3–10.
 258 ³D. G. Senesky, B. Jamshidi, K. B. Cheng, and A. P. Pisano, "Harsh environment
 259 silicon carbide sensors for health and performance monitoring of aerospace
 260 systems: A review," *IEEE Sens. J.* **9**, 1472–1478 (2009).
 261 ⁴N. Wright and A. Horsfall, "SiC sensors: A review," *J. Phys. D: Appl. Phys.* **40**,
 262 6345 (2007).

- 263 ⁵S. Rao, G. Pangallo, F. Pezzimenti, and F. G. Della Corte, “High-performance
264 temperature sensor based on 4H-SiC Schottky diodes,” *IEEE Electron Device*
265 *Lett.* **36**, 720–722 (2015). 278
- 266 ⁶P. G. Neudeck, “Progress in silicon carbide semiconductor electronics tech-
267 nology,” *J. Electron. Mater.* **24**, 283–288 (1995). 279
- 268 ⁷I. Josan, C. Boianceanu, G. Brezeanu, V. Obreja, M. Avram, D. Puscasu, and A.
269 Ioncea, “Extreme environment temperature sensor based on silicon carbide
270 Schottky diode,” in *International Semiconductor Conference (IEEE, 2009)*, Vol.
271 **2**, pp. 525–528. 280
- 272 ⁸N. R. Taylor, W. Kuang, M. Saeidijavash, P. Kandlakunta, Y. Zhang, and L. R.
273 Cao, “Direct printing of metal contacts on 4H-SiC for radiation detection,”
274 *AIP Adv.* **9**, 095041 (2019). 281
- 275 ⁹N. Zhang, C.-M. Lin, D. G. Senesky, and A. P. Pisano, “Temperature sensor
276 based on 4H-silicon carbide pn diode operational from 20 °C to 600 °C,” *Appl.*
277 *Phys. Lett.* **104**, 073504 (2014). 282
- ¹⁰S. Rao, G. Pangallo, and F. G. Della Corte, “Highly linear temperature sensor
based on 4H-silicon carbide p-i-n diodes,” *IEEE Electron Device Lett.* **36**,
1205–1208 (2015). 283
- ¹¹K. Hon, L. Li, and I. Hutchings, “Direct writing technology—Advances and
developments,” *CIRP Ann.* **57**, 601–620 (2008). 284
- ¹²S. Rao, G. Pangallo, L. D. Benedetto, A. Rubino, G. Licciardo, and F. Della
Corte, “Divanadium pentoxide/4H-silicon carbide: A Schottky contact for
highly linear temperature sensors,” *Procedia Eng.* **168**, 1003–1006 (2016). 285
- ¹³P. N. Luke, C. S. Tindall, and M. Amman, “Proximity charge sensing with semi-
conductor detectors,” *IEEE Trans. Nucl. Sci.* **56**, 808–812 (2009). 286
- ¹⁴R. Tung, “Electron transport at metal-semiconductor interfaces: General the-
ory,” *Phys. Rev. B* **45**, 13509 (1992). 287
- ¹⁵Y. Jiao, A. Hellman, Y. Fang, S. Gao, and M. Käll, “Schottky barrier formation
and band bending revealed by first-principles calculations,” *Sci. Rep.* **5**, 11374
(2015). 288
289
290
291
292